

# A Globally Convergent Adaptive Velocity Observer for Nonholonomic Mobile Robots Affected by Unknown Disturbances

Jose Guadalupe Romero<sup>1</sup> David Navarro-Alarcón<sup>2</sup> Emmanuel Nuño<sup>3</sup> Haoyi Que<sup>4</sup>

**Abstract**—In this paper, we present a novel adaptive observer for nonholonomic differential-drive robots to simultaneously estimate the system's angular and linear velocities, along with its external matched disturbances. The proposed method is based on the immersion and invariance technique and makes use of a dynamic scaling factor. The stability and convergence proof of the velocity and disturbance errors are performed using a strict Lyapunov function. We present a detailed simulation study to validate the performance of our approach.

**Index Terms**—Nonholonomic Robots; Velocity Observers; Adaptive Control; Disturbance Rejection.

## I. INTRODUCTION

WHEELED mobile robots are popular in many practical applications due to their control simplicity, lightness, flexibility, and capability to carry heavy loads. Yet, their nonholonomic constraints and nonlinear characteristics pose many complications to the development of stabilizing controllers, since (due to Brockett's theorem) nonholonomic systems cannot be stabilized using a smooth static feedback scheme [1].

Besides the mobility problems imposed by the nonholonomic constraints, the design of feedback controllers for real applications is also challenging since a controller may typically require access to the system's position and velocity measurements, which are often unavailable/unreliable. On-board inertial, encoders and vision sensors can be used to estimate the robot's position, however, velocity measurements are typically hard to obtain. The use of motion capture systems [2] and vision localization systems [3], among others, allows to numerically estimate velocity. However, this kind of signals are noisy and might contain errors, and, formally (as a result of unmodelled dynamics) these signals cannot be included in a rigorous stability analysis. The unified design of velocity

observers with feedback control represents a feasible solution to these issues.

In [4], a global exponentially convergent velocity observer is presented for general mechanical systems with nonholonomic constraints. The result is based on the well-known immersion and invariance (I&I) technique, which is a constructive methodology to design adaptive controllers and state observers for dynamical systems [5]. This breakthrough is possible due to a dynamic scaling that counteracts the undesired effects of nonlinear residual dynamics in the error equations—see also [6], [7]. Recently in [8], also using dynamic scaling to compensate for gyroscopic forces, an exponentially convergent velocity observer has been proposed. This result makes use of a special coordinate transformation that enables to convert a constrained system into an integral cascade Euler-Lagrange form; This eliminates the influence of the constraint force when the velocity is estimated.

Even though velocity estimation represents an key problem in nonholonomic robots, the most challenging issue is to take into account the presence of unknown parameters and disturbances in the design of an observer. Inspired by the methods in [4], [9], [10], an adaptive velocity observer that considers unknown external disturbances and friction parameters was proposed in [11]. The design of adaptive speed observers combined with a controller has been studied in several papers. For example, two high-gain observers with integrated control are proposed in [12] to estimate unknown parameters/velocities and ensure trajectory tracking. The method in [13] combines an adaptive velocity observer with backstepping control to ensure the asymptotic stability of estimation and tracking errors; This method compensates gyroscopic forces by using a coordinate transformation that guarantees the existence of the parameters' estimation. Although this design ensures the convergence of tracking errors, it is important to remark that it is based on the critical assumption that velocities are bounded, which cannot be verified in a rigorous stability analysis. Considering unknown input disturbances, [14] proposes a finite-time controller without velocity measurements, yet, the method relies on discontinuous velocity observers.

As a feasible solution to these problems, in this work, we propose a novel globally convergent adaptive velocity observer for nonholonomic robots subject to unknown input disturbances. The design does not rely on the use of high gains or discontinuous techniques, nor it assumes the

<sup>1</sup> Departamento Académico de Sistemas Digitales, ITAM. Ciudad de México, México. email: jose.romerovelazquez@itam.mx

<sup>2</sup> Department of Mechanical Engineering, The Hong Kong Polytechnic University (PolyU), KLN, Hong Kong. email: dna@ieee.org

<sup>3</sup> Department of Computer Science, CUCEI. University of Guadalajara, Guadalajara, Mexico. email: emmanuel.nuno@cucei.udg.mx

<sup>4</sup> Department of Control Science & Engineering, Zhejiang University, Hangzhou, China. email: hyque@zju.edu.cn

The work of E. Nuño is supported by the Government of Mexico via the Basic Scientific Research grant CB-282807, sponsored by CONA-CyT, and by the Government of Spain through the project PID2020-114819GB-I00.

boundedness of velocity signals. An interesting feature of our proposal is that the adaptive observer can exactly estimate the input disturbance. In contrast with existing methods, our new methodology simplifies the implementation of adaptive velocity observers, as only continuous control signals are needed. The stability analysis is rigorously established using Lyapunov theory. Furthermore, in comparison with [4], our work has the following two key features: a) The nonholonomic dynamic model [4] does not consider the presence of external disturbances. Hence, its observer fails to estimate the velocities when disturbance is present; and b) The convergence proof in [4] has been carried out using a dynamic scaling factor in both, linear and angular velocities, which contrasts with our result, where only requires the linear part. Moreover, our stability analysis ensures also the estimation of the disturbances, which is conspicuous by its absence in [4], where its consideration would require additional definitions in the dynamics of the observer.

The rest of the paper is organized as follows: Section II presents the dynamic model of the nonholonomic robot; Section III contains our main result; and, finally, the simulations and conclusions are shown in Sections IV and V, respectively.

## II. MATHEMATICAL MODEL

In this work we consider a differential wheeled mobile robot moving on the horizontal plane, for which we assume that the geometrical center and the center of mass are located at the same point  $z = \text{col}(x, y) \in \mathbb{R}^2$  and  $\theta \in \mathbb{R}$  defining its orientation. The schematics of this robot is depicted in Fig. 1. Under the common non-slip (pure rolling) assumption, the robot dynamics takes the form

$$\begin{aligned} \dot{z} &= \begin{bmatrix} \cos(\theta) \\ \sin(\theta) \end{bmatrix} v, \quad \dot{\theta} = \omega, \\ \begin{bmatrix} \dot{v} \\ \dot{\omega} \end{bmatrix} &= M^{-1} \mathcal{B}(\tau + d), \end{aligned} \quad (1)$$

where  $v$  and  $\omega$  are the linear and the angular velocities;  $M := \text{diag}(m, I) \in \mathbb{R}^2$  is the inertia matrix with  $I$  being the moment of inertia and  $m$  being the mass;  $\mathcal{B}$  is the input matrix given by

$$\mathcal{B} = \frac{1}{r} \begin{bmatrix} 1 & 1 \\ 2R & -2R \end{bmatrix} \quad (2)$$

with  $R$  being the distance between  $z$  and the wheels which have radius  $r$ ; the control signal of the wheels is  $\tau \in \mathbb{R}^2$  and  $d \in \mathbb{R}^2$  is a constant *unknown* disturbance [15], [16].

Making simple calculations we have that model (1) can be written in a cascaded form, of the linear and the angular dynamics, as follows

$$\Sigma_\omega \quad \begin{cases} \dot{\theta} = \omega \\ \dot{\omega} = u_2 + \delta_2 \end{cases} \quad (3)$$

$$\Sigma_v \quad \begin{cases} \dot{z} = h(\theta)v \\ \dot{v} = u_1 + \delta_1, \end{cases} \quad (4)$$

where  $h(\theta) = \text{col}(\cos(\theta), \sin(\theta)) \in \mathbb{R}^2$ ;  $u_1$  and  $u_2$  are the control-input signals, given by

$$u_1 = \frac{1}{mr}(\tau_1 + \tau_2), \quad u_2 = \frac{2R}{Ir}(\tau_1 - \tau_2),$$

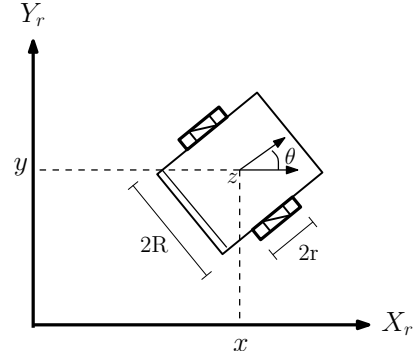


Fig. 1. Schematics of a differential wheeled mobile robot

and the *unknown* constant disturbances  $\delta_1$  and  $\delta_2$ , are

$$\delta_1 := \frac{1}{mr}(d_1 + d_2), \quad \delta_2 := \frac{2R}{Ir}(d_1 - d_2), \quad (5)$$

respectively.

## III. MAIN RESULT

The objective of this work is to design an adaptive observer that is able to globally estimate the linear and the angular velocities together with the external disturbances. For, the following assumption is employed.

**Assumption 1.** The orientation and the position of the robot are available for measurement, i.e.,  $\theta$  and  $z$  are known.  $\triangleleft$

Our solution follows the Immersion and Invariance (I&I) methodology proposed in [5]—see also [4], [17]. First, we define the estimation errors as

$$\begin{aligned} \bar{v} &= \hat{v} - v, \quad \bar{\omega} = \hat{\omega} - \omega, \quad \bar{\theta} = \hat{\theta} - \theta \\ \bar{\delta}_1 &= \hat{\delta}_1 - \delta_1, \quad \bar{\delta}_2 = \hat{\delta}_2 - \delta_2, \end{aligned} \quad (6)$$

where  $\hat{\omega}$ ,  $\hat{v}$ ,  $\hat{\theta}$ ,  $\hat{\delta}_1$  and  $\hat{\delta}_2$  are the estimations of the linear and the angular velocities, of the orientation and of the disturbances, respectively. In the I&I technique, the adaptive observer consists of two parts, an integral and a proportional. Therefore, the estimations are similarly defined as

$$\begin{aligned} \hat{v} &= v_I + v_P(\hat{\theta}, z), \quad \hat{\omega} = \omega_I + \omega_P(\hat{\theta}) \\ \hat{\delta}_1 &= \delta_{1I} + \delta_{1P}(z, \hat{\theta}), \quad \hat{\delta}_2 = \delta_{2I} + \delta_{2P}(\theta). \end{aligned} \quad (7)$$

Under **Assumption 1** above, the main objective in the observer design is to find the dynamics of the integral terms  $v_I$ ,  $\omega_I$ ,  $\delta_{1I}$ ,  $\delta_{2I}$ ; and to set the proportional parts  $v_P$ ,  $\omega_P$ ,  $\delta_{1P}$ ,  $\delta_{2P}$ ; such that the estimation errors (6) exponentially converge to zero for all initial conditions.

At this point, we are ready to present our main result.

**Proposition 1:** Consider the subsystems  $\Sigma_\omega$  and  $\Sigma_v$  given by (3) and by (4), respectively. Define the integral dynamics

of (7) and the  $\hat{\theta}$ -dynamics as<sup>1</sup>

$$\dot{v}_I = -a_3 h^\perp(\hat{\theta}) z \dot{\hat{\theta}} - a_3 h^\top(\hat{\theta}) h(\theta) \hat{v} + u_1 + \hat{\delta}_1, \quad (8)$$

$$\dot{\omega}_I = -a_1 \hat{\omega} + u_2 + \hat{\delta}_2, \quad (9)$$

$$\dot{\delta}_{1I} = -a_4 h^\perp(\hat{\theta}) z \dot{\hat{\theta}} - a_4 h^\top(\hat{\theta}) h(\theta) \hat{v}, \quad (10)$$

$$\dot{\delta}_{2I} = -a_2 \hat{\omega}, \quad (11)$$

$$\dot{\hat{\theta}} = \hat{\omega} - k_a(r_v) \bar{\theta}, \quad (12)$$

where  $r_v$  is obtained from a dynamic scaling that is defined latter. Additionally, set the proportional terms to

$$\omega_P = a_1 \theta, \quad v_P = a_3 z^\top h(\hat{\theta}), \quad (13)$$

$$\delta_{1P} = a_4 z^\top h(\hat{\theta}), \quad \delta_{2P} = a_2 \theta. \quad (14)$$

The gains  $a_i$ , for  $i = 1 : 4$ , and  $k_1$  are free to choose. Then, provided that  $k_a(r_v) > 0$  is sufficiently large, for all initial conditions  $(z(0), \theta(0), v(0), \omega(0)) \in \mathbb{R}^2 \times \mathbb{R} \times \mathbb{R} \times \mathbb{R}$ , we ensure that

$$\lim_{t \rightarrow \infty} (\bar{v}(t), \bar{\omega}(t), \bar{\delta}_1(t), \bar{\delta}_2(t), \bar{\theta}(t)) = 0. \quad (15)$$

*Proof:* We start by analyzing the adaptive observer for the subsystem  $\Sigma_\omega$ . The dynamic behavior of  $\bar{\omega}$  is given by

$$\dot{\bar{\omega}} = \dot{\omega}_I + a_1(\hat{\omega} - \bar{\omega}) - u_2 - (\hat{\delta}_2 - \bar{\delta}_2).$$

Choosing  $\dot{\omega}_I$  as in (9), yields

$$\dot{\bar{\omega}} = -a_1 \bar{\omega} + \bar{\delta}_2. \quad (16)$$

Besides, the dynamic behavior of  $\bar{\delta}_2$  corresponds to

$$\dot{\bar{\delta}}_2 = \dot{\delta}_{2I} + a_2(\hat{\omega} - \bar{\omega}). \quad (17)$$

Hence, selecting  $\dot{\delta}_{2I}$  as (11), the error dynamics takes the form

$$\dot{\bar{\delta}}_2 = -a_2 \bar{\omega}. \quad (18)$$

We can notice that the error dynamics (16) and (18) can be rewritten as

$$\begin{bmatrix} \dot{\bar{\omega}} \\ \dot{\bar{\delta}}_2 \end{bmatrix} = \begin{bmatrix} -a_1 & 1 \\ -a_2 & 0 \end{bmatrix} \begin{bmatrix} \bar{\omega} \\ \bar{\delta}_2 \end{bmatrix}. \quad (19)$$

Consider the Lyapunov function

$$\bar{H}_\omega = \frac{1}{2} \mathcal{X}^\top \begin{bmatrix} \gamma_1 & \gamma_2 \\ \gamma_2 & \gamma_1 \end{bmatrix} \mathcal{X}, \quad (20)$$

with  $\mathcal{X} = \text{col}(\bar{\omega}, \bar{\delta}_2)$  and  $\gamma_1 > \gamma_2 > 0$ . Evaluating  $\dot{\bar{H}}_\omega$  along the solutions (19), yields,

$$\dot{\bar{H}}_\omega = -\mathcal{X}^\top \begin{bmatrix} \sigma_1 & \sigma_2 \\ \sigma_2 & \gamma_2 \end{bmatrix} \mathcal{X} \quad (21)$$

with

$$\sigma_1 = a_1 \gamma_1 - a_2 \gamma_2, \quad (22)$$

$$\sigma_2 = \frac{1}{2} [\gamma_1(a_2 - 1) - a_1 \gamma_2]. \quad (23)$$

<sup>1</sup> $h(\hat{\theta}) = \text{col}(\cos(\hat{\theta}), \sin(\hat{\theta}))$  and  $h^\perp(\hat{\theta}) = [-\sin(\hat{\theta}), \cos(\hat{\theta})]$ , being  $h^\perp(\cdot)$  a full-rank left annihilator of  $h(\cdot)$ , which verifies  $h^\perp(\cdot)h(\cdot) = 0$ .

Now, to impose  $\sigma_2 = 0$ , we set

$$\gamma_2 = \gamma_1 \frac{(a_2 - 1)}{a_1}. \quad (24)$$

Since we need to verify  $\gamma_1 > \gamma_2$ , the elements  $a_1$  and  $a_2$  are chosen such that  $a_1 > a_2 - 1$ . Thus, (21) takes the form

$$\dot{\bar{H}}_\omega = -\sigma_1 \bar{\omega}^2 - \gamma_2 \bar{\delta}_2^2. \quad (25)$$

Finally, (25) is negative definitive if  $\sigma_1 > 0$ . Then, using definition of  $\sigma_1$  we have the following implication

$$a_1 \gamma_1 > a_2 \gamma_2 \Rightarrow \gamma_1 > \gamma_2 \frac{a_2}{a_1}. \quad (26)$$

Invoking (24) and also imposing  $0 < \frac{a_2}{a_1} \leq 1$ , we prove that  $\sigma_1 > 0$ . Thus, from (20) and (25) we establish that  $\bar{\omega}, \bar{\delta}_2 \in \mathcal{L}_2 \cap \mathcal{L}_\infty$  and that  $(\bar{\omega}, \bar{\delta}_2) = (0, 0)$  is globally asymptotically stable.

We now study the adaptive observer for the subsystem  $\Sigma_v$ . Taking the time derivative of  $\bar{v}$ , we obtain

$$\begin{aligned} \dot{\bar{v}} &= \dot{v}_I + a_3(z^\top \nabla h(\hat{\theta}) \dot{\hat{\theta}} + h^\top(\hat{\theta}) \dot{z}) - \dot{v} \\ &= \dot{v}_I + a_3 h^\perp(\hat{\theta}) z \dot{\hat{\theta}} + a_3 h^\top(\hat{\theta}) h(\theta) [\hat{v} - \bar{v}] \\ &\quad - u_1 - (\hat{\delta}_1 - \bar{\delta}_1). \end{aligned} \quad (27)$$

Choosing  $\dot{v}_I$  as in (8), we get

$$\dot{\bar{v}} = -a_3 h^\top(\hat{\theta}) h(\theta) \bar{v} + \bar{\delta}_1, \quad (28)$$

which can be written as

$$\begin{aligned} \dot{\bar{v}} &= -a_3 \bar{v} - a_3 \Delta_v(\hat{\theta}, \theta) \bar{v} + \bar{\delta}_1, \\ \Delta_v(\hat{\theta}, \theta) &:= [h^\top(\hat{\theta}) - h^\top(\theta)] h(\theta), \end{aligned} \quad (29)$$

where we have used the fact that  $h^\top(\theta) h(\theta) = 1$  and

$$\begin{aligned} h^\top(\hat{\theta}) h(\theta) &= [h^\top(\hat{\theta}) \pm h^\top(\theta)] h(\theta) \\ &:= 1 + \Delta_v(\hat{\theta}, \theta). \end{aligned} \quad (30)$$

It is important to note that  $\Delta_v = 0$ , if  $\bar{\theta} = 0$ , and that

$$\|\Delta_v(\hat{\theta}, \theta)\| \leq 2\bar{\theta}. \quad (31)$$

As a consequence,  $\Delta_v$  plays the role of a (vanishing) disturbance that will be dominated though a dynamic scaling factor and a proper choice of the  $\hat{\theta}$  dynamics.

Using the definition of  $\hat{\delta}_1$ , the time derivative of  $\bar{\delta}_1$  is

$$\begin{aligned} \dot{\bar{\delta}}_1 &= \dot{\delta}_{1I} + a_4 \left( z^\top \nabla h(\hat{\theta}) \dot{\hat{\theta}} + h^\top(\hat{\theta}) \dot{z} \right) \\ &:= \dot{\delta}_{1I} + a_4 h^\top(\hat{\theta}) h(\theta) (\hat{v} - \bar{v}) + a_4 h^\perp(\hat{\theta}) z \dot{\hat{\theta}}. \end{aligned} \quad (32)$$

Selecting  $\dot{\delta}_{1I}$  as in (10) and using (30), we obtain

$$\dot{\bar{\delta}}_1 = -a_4 \bar{v} - a_4 \Delta_v(\hat{\theta}, \theta) \bar{v}. \quad (33)$$

Defining  $\zeta = \text{col}(\bar{v}, \bar{\delta}_1)$ , the dynamics (29) and (33) are rewritten as

$$\dot{\zeta} = A_v \zeta + \Delta_v M_v \zeta \quad (34)$$

with

$$A_v = \begin{bmatrix} -a_3 & 1 \\ -a_4 & 0 \end{bmatrix}, \quad M_v = \begin{bmatrix} -a_3 & 0 \\ -a_4 & 0 \end{bmatrix}. \quad (35)$$

Since  $A_v$  is a Hurwitz matrix, then there exists a transformation for  $A_v$  such that  $\mathcal{R} := EA_vE^{-1} = \text{diag}(\lambda_1, \lambda_2)$ , where  $E \in \mathbb{R}^{2 \times 2}$  is a full rank matrix and  $\lambda_i \in \mathbb{R}_-$  are the eigenvalues of  $A_v$  for  $i = 1 : 2$ , which are given by

$$\lambda_1 = -\frac{a_3}{2} + \frac{\sqrt{a_3^2 - 4a_4}}{2}, \quad \lambda_2 = -\frac{a_3}{2} - \frac{\sqrt{a_3^2 - 4a_4}}{2}.$$

Let us define the following dynamically scaling

$$z_v = \frac{1}{r_v} E \zeta, \quad (36)$$

with  $r_v$  being a *scaling dynamic* factor, with dynamics defined as

$$\dot{r}_v := -\frac{k_1}{4} \bar{r}_v + \frac{r_v}{2k_1} \|\Delta_v \mathcal{M}\|^2, \quad r_v(0) > 1, \quad (37)$$

where  $\bar{r}_v(t) = r_v(t) - 1$  and  $\mathcal{M} = EME^{-1}$ . Notice that the set  $\{r_v \in \mathbb{R} | r_v \geq 0\}$  is invariant for the dynamics (37).

The dynamics of  $z_v$ , defined in (36) yields

$$\begin{aligned} \dot{z}_v &= \frac{1}{r_v} E \dot{\zeta} - \frac{\dot{r}_v}{r_v^2} E \zeta \\ &= \mathcal{R} z_v + \Delta_v \mathcal{M} z_v - \frac{\dot{r}_v}{r_v} z_v. \end{aligned} \quad (38)$$

In addition, the  $\bar{\theta}$  dynamics corresponds to

$$\dot{\bar{\theta}} = \dot{\theta} - (\hat{\omega} - \bar{\omega}) := -k_a \bar{\theta} + \bar{\omega}, \quad (39)$$

where we have chosen  $\dot{\bar{\theta}}$  as in (12).

Consider now the Lyapunov function

$$H_z = \bar{H}_w + \frac{1}{2} (|z_v|^2 + \bar{\theta}^2 + \bar{r}_v^2). \quad (40)$$

Taking its time derivative along the dynamics (19), (38) and (39), we get

$$\begin{aligned} \dot{H}_z &= -\sigma_1 \bar{\omega}^2 - \gamma_2 \bar{\delta}_2^2 + z_v^\top \left( \mathcal{R} + \Delta_v(\theta, \hat{\theta}) \mathcal{M} - \frac{\dot{r}_v}{r_v} \right) z_v \\ &\quad - k_a \bar{\theta}^2 + \bar{\theta} \bar{\omega} + \dot{r}_v \bar{r}_v \\ &\leq -\sigma_1 \bar{\omega}^2 - \gamma_2 \bar{\delta}_2^2 - \left( \frac{k_1}{2} - \frac{1}{2k_1} \|\Delta_v \mathcal{M}\|^2 + \frac{\dot{r}_v}{r_v} \right) |z_v|^2 \\ &\quad - k_a \bar{\theta}^2 + \frac{1}{2} \bar{\theta}^2 + \frac{1}{2} \bar{\omega}^2 + \dot{r}_v \bar{r}_v, \end{aligned} \quad (41)$$

where  $k_1 = -\max(\lambda_1, \lambda_2)$ ,  $\|\cdot\|$  is the matrix induced 2-norm and we have applied Young's inequality (with the factor  $k_1$ ) to get the second bound. Using (37) and making use of (31), we get

$$\begin{aligned} \dot{H}_z &\leq -\left( \sigma_1 - \frac{1}{2} \right) \bar{\omega}^2 - \gamma_2 \bar{\delta}_2^2 - k_1 \left( \frac{1}{2} - \frac{\bar{r}_v}{4r_v} \right) |z_v|^2 \\ &\quad - \left( k_a - \frac{1}{2} - 2 \frac{\bar{r}_v r_v}{k_1} \|\mathcal{M}\|^2 \right) \bar{\theta}^2 - \frac{k_1}{4} \bar{r}_v^2, \\ &\leq -k_x \bar{\omega}^2 - \gamma_2 \bar{\delta}_2^2 - \frac{k_1}{4} |z_v|^2 - k_y \bar{\theta}^2 - \frac{k_1}{4} \bar{r}_v^2 \end{aligned} \quad (42)$$

where the last inequality has been obtained using the fact that  $0 < \frac{\bar{r}_v}{r_v} \leq 1$  and selected  $a_1, a_2$ , such that  $\sigma_1 = k_x + \frac{1}{2}$  and we have defined  $k_a(r_v)$  as

$$k_a(r_v) = k_y + \frac{1}{2} + \frac{2}{k_1} \bar{r}_v r_v \|\mathcal{M}\|^2. \quad (43)$$

Thus, from (40) and (42) we ensure that  $\bar{\omega}, \bar{\delta}_2, z_v, \bar{\theta}, \bar{r}_v \in \mathcal{L}_2 \cap \mathcal{L}_\infty$ . This last ensures that  $\dot{H}_z$  is uniformly bounded and thus, invoking Barbalat's Lemma, we conclude that  $\dot{H}_z$  converges to zero as  $t \rightarrow \infty$ . The proof is finished with the fact that  $\dot{H}_z$  only vanishes when  $\bar{\omega}, \bar{\delta}_2, z_v, \bar{\theta}$  and  $\bar{r}_v$  are all equal to zero. ■

The following remarks are in order.

- I) Although, the stability conclusion is asymptotical, we underscore that the the unique solution of the error dynamics (19) is  $\mathcal{X}(t) = e^{\mathcal{D}t} \mathcal{X}(0)$ , which ensures exponential convergence to zero of  $\mathcal{X}(t)$ .
- II) The subsystem  $\Sigma_\omega$  is equivalent to the dynamics of a (general) rotating machine model with  $\delta_2$  being the load torque. In [18] an adaptive observer for such a system is proposed. In contrast with such result, our adaptive velocity observer has a simpler form. However, the insightful idea of diagonalizing a Hurwitz matrix to define dynamic scaling (see eq. (17) of [18]) is used in our stability analysis for the subsystem  $\Sigma_v$ .

#### IV. SIMULATIONS

In this section we present simulations of the proposed adaptive observer under two scenarios: an open-loop estimation and a closed-loop observer-controller scheme. The simulation parameters are  $m = 5.64$  kg,  $I = 3.115$  kg·m<sup>2</sup>,  $r = 0.09$  m and  $R = 0.157$  m.

##### A. Open loop estimation

To evaluate the robustness of the adaptive velocity observer, we consider that the input disturbance  $d_1$  and  $d_2$  are subject to step changes, as shown in Fig. 2—which imply that they are time varying. We carried out the simulation using as input signal

$$\tau = \mathcal{B}^{-1} M \begin{bmatrix} -k_x h^\top(\theta) z \\ -k_c \theta \end{bmatrix}$$

with  $k_x = 0.6$  and  $k_c = 6$ . The adaptive observer gains are chosen as  $a_1 = 3$  and  $a_2 = 2$ , verifying the conditions (24) and (26),  $a_3 = 5$ ,  $a_4 = 3$ , so that  $k_1 = -4.3028$ ,

$$E = \begin{bmatrix} -1.4548 & 0.3381 \\ 0.8542 & -1.2252 \end{bmatrix}$$

and  $k_y = 3.5$ . The initial conditions were selected as  $\theta(0) = 0.5$ ,  $\omega(0) = 0$ ,  $z(0) = \text{col}(0.5, 0)$ ,  $v(0) = 0$ ,  $\omega_I(0) = 0.5$ ,  $v_I = 0.5$ ,  $\delta_{1I}(0) = 1.5$ ,  $\delta_{2I}(0) = -0.5$ ,  $\hat{\theta}(0) = 0.5$ ,  $r_v(0) = 3.5$ . Since the proposed estimator is globally convergent, the choice of these initial conditions were arbitrary.

Clearly, from Figs. 3–4, the transient behavior of the estimator errors corroborative the proposed theory. Moreover, since we use *time varying* disturbances, the adaptive observer presents an overshoot every time the disturbance changes, but the estimation is preserved, which shows its robustness. Besides, from (5) we notice that the *real value* of the disturbances  $d_1$  and  $d_2$  can be estimated using  $\hat{\delta}_1$  and  $\hat{\delta}_2$  as follows  $\text{col}(\hat{d}_1, \hat{d}_2) = \mathcal{B}^{-1} M \text{col}(\hat{\delta}_1, \hat{\delta}_2)$ . Thus, in Fig. 5 we also appreciate the estimation of the time varying disturbances proposed in Fig. 2.

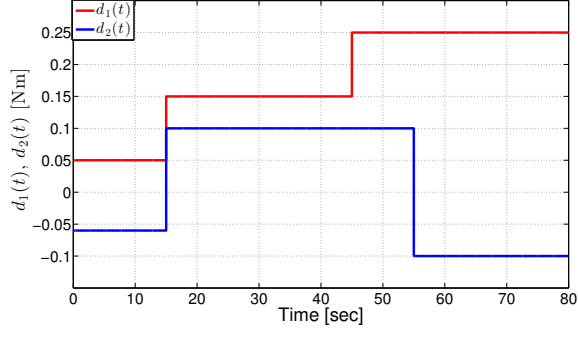


Fig. 2. Transient behavior of  $d_1(t)$  and  $d_2(t)$

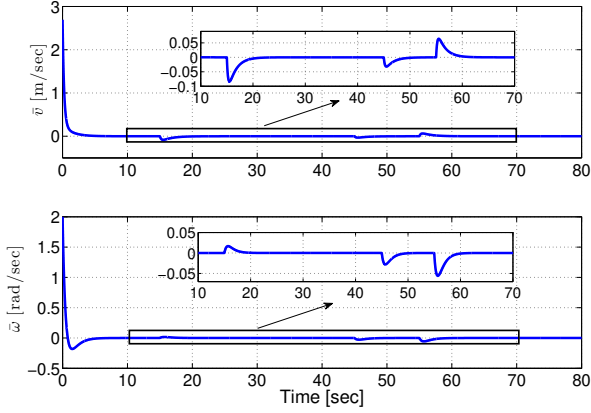


Fig. 3. Transient behavior of  $\bar{v}$  and  $\bar{\omega}$

### B. Closed loop controller

Our second series of simulations pertains to the implementation of an adaptive velocity observer based controller of the form

$$\begin{aligned} u_1 &= -p_v h(\theta)^\top \tilde{z} - d_v \hat{v} - \hat{\delta}_1, \\ u_2 &= -p_\omega \tilde{\theta} - d_\omega \hat{\omega} - \hat{\delta}_2 + K_I f(t) h(\theta)^\perp \tilde{z}, \end{aligned} \quad (44)$$

where

$$\tilde{z}(t) = z(t) - z_d \quad \tilde{\theta}(t) = \theta(t) - \theta_d.$$

with  $z_d \in \mathbb{R}^2$  and  $\theta_d$  as the desired position and orientation, respectively and; control gains  $p_v$ ,  $d_v$ ,  $p_\omega$ ,  $d_\omega$  and  $K_I$ .

This controller ensures *asymptotic* convergence to a desired point of both position and angular coordinates. The control law has a simple PD structure plus the estimator of the disturbances and a time varying term  $f(t)$  which verifies the Brockett's condition. To the best knowledge of the authors, this adaptive velocity observer based controller has not been reported in the literature and all details of the stability proof will be reported later.

In order to carry out the simulations we consider as input disturbances  $d = \text{col}(0.07, -0.0193)Nm$ , then (5) takes the form  $\text{col}(\delta_1, \delta_2) = 0.1I_2$ . In Figs. 6 and 7 we appreciate the convergence to zero of the coordinate errors, where the initial conditions are  $z(0) = (0.1, 0.2)m$  and  $\theta(0) = 0.5rad$  and the desired point  $z_d = (4, 3)m$  and  $\theta_d = -\frac{\pi}{6}$ . Figs. 8

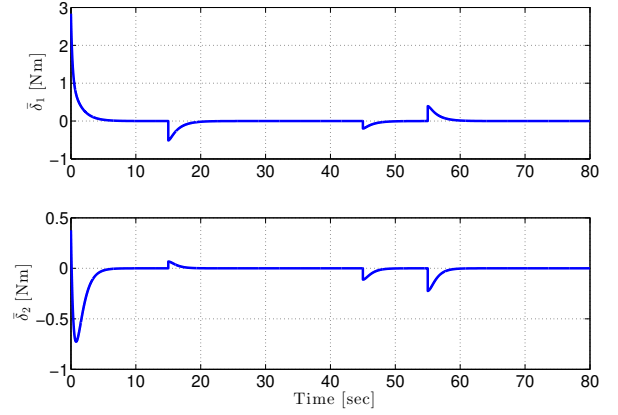


Fig. 4. Transient behavior of  $\bar{\delta}_1$  and  $\bar{\delta}_2$

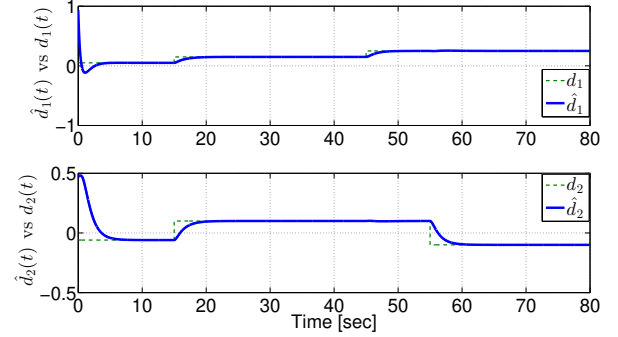


Fig. 5. Transient behavior of  $d_1(t)$  vs  $\hat{d}_1(t)$  and  $d_2(t)$  vs  $\hat{d}_2(t)$

and 9 show the transient behavior of the velocity estimator and disturbances errors, respectively—as the open-loop case—the estimation is also ensured. Finally, since the convergence to zero of the coordinates errors hold, the input control compensate the constant disturbance, this effect is appreciate in Fig. 10, where we notice that  $\tau$  converges to  $-d$ .

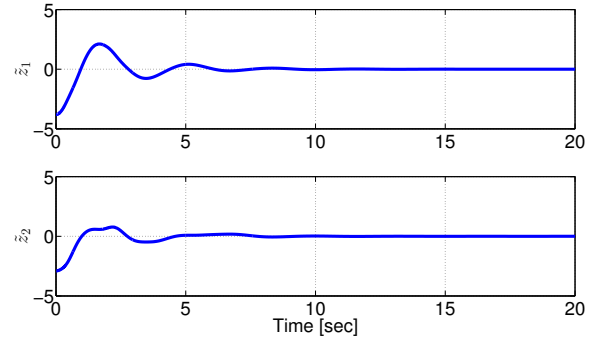


Fig. 6. Transient behavior of the position errors  $\tilde{z}$

## V. CONCLUSIONS

We have presented a procedure to design a globally convergent adaptive velocity observer for nonholonomic mobile robots with unknown input disturbances. The rigorous stability analysis is established using Lyapunov theory. The adaptive



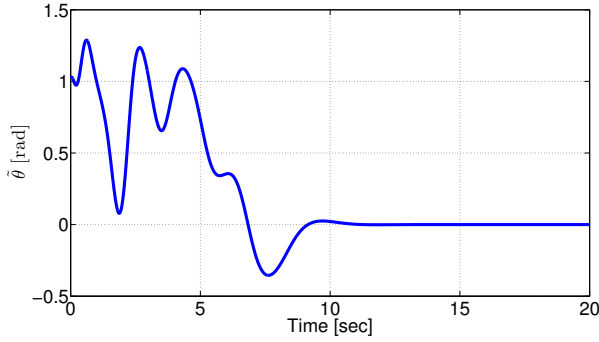


Fig. 7. Transient behavior of the angular error  $\tilde{\theta}$

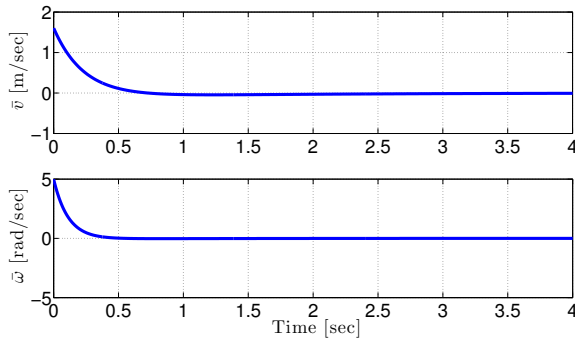


Fig. 8. Transient behavior of  $\bar{v}$  and  $\bar{\omega}$  using the controller (44)

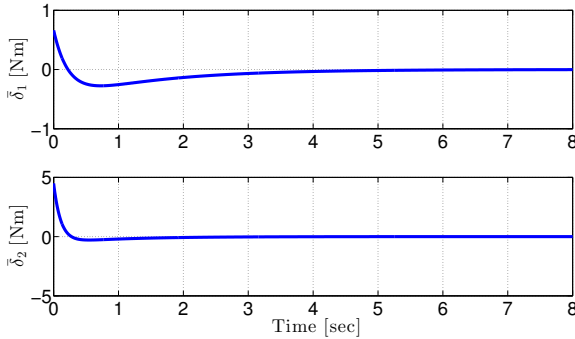


Fig. 9. Transient behavior of  $\bar{\delta}_1$  and  $\bar{\delta}_2$  using the controller (44)

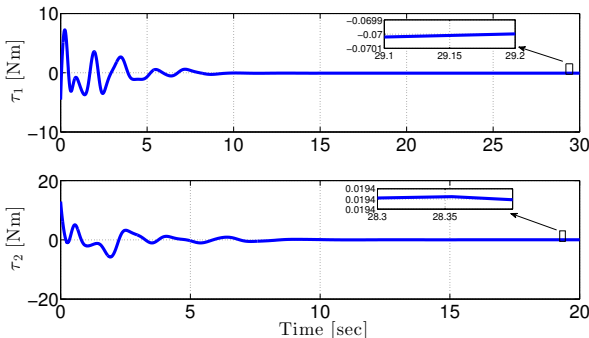


Fig. 10. Transient behavior of the input controller  $\tau$

observer is tested by simulations which show its satisfactory performance. Even though the observer has been designed considering constant input disturbances, the simulations show its robustness under time varying disturbances. In addition, making use of the proposed adaptive velocity observer, we simulate an output feedback controller to stabilise the robot at a desired point and, as expected, the convergence to zero of position error and of velocity and disturbance estimation errors is ensured. As future work we will present the stability analysis of the observer in closed-loop with the controller mentioned in the simulations.

## REFERENCES

- [1] R. W. Brockett, "Asymptotic stability and feedback stabilization," *Differential geometric control theory*, vol. 27, no. 1, pp. 181–191, 1983.
- [2] S. Dudzik, "Application of the motion capture system to estimate the accuracy of a wheeled mobile robot localization," *Energies*, vol. 13, no. 23, pp. 1–23, 2020.
- [3] P. Dutkiewicz, M. Kielczewski, K. Kozłowski, and D. Pazderski, "Vision localization system for mobile robot with velocities and acceleration estimator," *Bulletin of the Polish Academy of Sciences and Technical Sciences*, vol. 58, no. 1, pp. 1–14, 2010.
- [4] A. Astolfi, R. Ortega, and A. Venkatraman, "A globally exponentially convergent immersion and invariance speed observer for mechanical systems with non-holonomic constraints," *Automatica*, vol. 46, no. 1, pp. 182–189, 2010.
- [5] A. Astolfi, D. Karagiannis, and R. Ortega, *Nonlinear and adaptive control with applications*. Springer, 2008.
- [6] A. Astolfi and R. Ortega, "Immersion and invariance: a new tool for stabilization and adaptive control of nonlinear systems," *IEEE Transactions on Automatic Control*, vol. 48, no. 4, pp. 590–606, 2003.
- [7] J. G. Romero, R. Ortega, and I. Sarra, "A globally exponentially stable tracking controller for mechanical systems using position feedback," *IEEE Transactions on Automatic Control*, vol. 60, no. 3, pp. 818–823, 2015.
- [8] L. Liu, X. Yue, H. Wen, S. Tian, and D. Zhao, "Globally exponentially convergent velocity observer design for mechanical systems with non-holonomic constraints," *International Journal of Robust and Nonlinear Control*, vol. 32, no. 2, pp. 851–872, 2022.
- [9] J. G. Romero and R. Ortega, "Two globally convergent adaptive speed observers for mechanical systems," *Automatica*, vol. 60, no. 1, pp. 7–11, 2015.
- [10] J. G. Romero, J. Moreno, and A. A. Maradiaga-Aguilar, "An adaptive speed observer for a class of nonlinear mechanical systems: Theory and experiments," *Automatica*, vol. 130, 2021.
- [11] A. T. Brahim and M. Kidouche, "A constructive globally convergent adaptive speed observer for port-hamiltonian mechanical systems with non-holonomic constraints," *Asian Journal of Control*, vol. 21, no. 2, pp. 965–976, 2019.
- [12] J. Huang, C. Wen, W. Wang, and Z. Jiang, "Adaptive output feedback tracking control of a nonholonomic mobile robot," *Automatica*, vol. 50, no. 1, pp. 821–831, 2014.
- [13] B. S. Park, J. Park, and Y. H. Choi, "Adaptive observer-based trajectory tracking control of nonholonomic mobile robots," *International Journal of Control, Automation, and Systems*, vol. 9, pp. 534–541, 2011.
- [14] S. Shi, X. Yu, and S. S. Khoo, "Robust finite-time tracking control of nonholonomic mobile robots without velocity measurements," *International Journal of Control*, vol. 89, no. 2, pp. 411–423, 2016.
- [15] S. G. Tzafestas, *Introduction to mobile robot control*. Elsevier, 2013.
- [16] A. Donaïre, J. G. Romero, T. Perez, and R. Ortega, "Smooth stabilization of nonholonomic robots subject to disturbances," in *2015 IEEE International Conference on Robotics and Automation (ICRA)*, 2015, pp. 4385–4390.
- [17] J. G. Romero and E. Nuño, "Global stabilization of nonholonomic mobile robots via a smooth output feedback time-varying controller," in *2019 IEEE 15th International Conference on Control and Automation (ICCA)*, 2010, pp. 393–398.
- [18] D. Shah, R. Ortega, and A. Astolfi, "Speed and load torque observer for rotating machines," in *48th IEEE Conference on Decision and Control*, 2009, pp. 6143–6148.